A Locomotion Mode Recognition Algorithm Using Adaptive Dynamic Movement Primitives

Huseyin Eken, *Graduate Student Member, IEEE*, Francesco Lanotte, *Member, IEEE*, Vito Papapicco, Michele Francesco Penna, Emanuele Gruppioni, *Member, IEEE*, Emilio Trigili, *Member, IEEE*, Simona Crea, *Member, IEEE*, and Nicola Vitiello, *Member, IEEE*

***Abstract*— Control systems of robotic prostheses should be designed to decode the users' intent to start, stop, or change locomotion; and to select the suitable control strategy, accordingly. This paper describes a locomotion mode recognition algorithm based on adaptive Dynamic Movement Primitive models used as locomotion templates. The models take foot-ground contact information and thigh roll angle, measured by an inertial measurement unit, for generating continuous model variables to extract features for a set of Support Vector Machines. The proposed algorithm was tested offline on data acquired from 10 intact subjects and 1 subject with transtibial amputation, in ground-level walking and stair ascending/descending activities. Following subject-specific training, results on intact subjects showed that the algorithm can classify initiatory and steady-state steps with up to 100.00% median accuracy medially at 28.45% and 27.40% of the swing phase, respectively. While the transitory steps were classified with up to 87.30% median accuracy medially at 90.54% of the swing phase. Results with data of the transtibial amputee showed that the algorithm classified initiatory, steady-state, and transitory steps with up to 92.59%, 100%, and 93.10% median accuracies medially at 19.48%, 51.47%, and 93.33% of the swing phase, respectively. The results support the feasibility of this approach in robotic prosthesis control.**

***Index Terms*— Movement primitives, inertial measurement unit, intention decoding, support vector machines, wearable robotics.**

Manuscript received 3 May 2023; revised 30 August 2023 and 9 October 2023; accepted 22 October 2023. Date of publication 26 October 2023; date of current version 7 November 2023. This work was supported by Istituto Nazionale Assicurazione Infortuni sul Lavoro (Inail) within the MOTU++ Project PR19-PAI-P2. *(Corresponding author: Huseyin Eken.)*

This work involved human subjects in its research. Approval of all ethical and experimental procedures and protocols was granted by the Institutional Review Board of Sant'Anna School of Advanced Studies for the intact subjects under Approval No. 11/2019 and the Area Vasta Toscana Centro Ethics Committee for the amputee subject under Approval No. 16678, and performed in line with the Declaration of Helsinki.

Huseyin Eken, Michele Francesco Penna, and Emilio Trigili are with The BioRobotics Institute, Scuola Superiore Sant'Anna, 56025 Pontedera, Italy, and also with the Department of Excellence in Robotics and AI, Scuola Superiore Sant'Anna, 56127 Pisa, Italy (e-mail: huseyin.eken@santannapisa.it).

Francesco Lanotte was with The BioRobotics Institute, 56025 Pontedera, Italy. He is now with the Department of Physical Medicine and Rehabilitation, Northwestern University, Chicago, IL 60611 USA, and also with the Max Nader Laboratory for Rehabilitation Technologies and Outcomes Research and the Shirley Ryan AbilityLab, Chicago, IL 60611 USA.

Vito Papapicco was with The BioRobotics Institute, 56025 Pontedera, Italy.

Emanuele Gruppioni is with Centro Protesi Inail di Vigorso di Budrio, 40054 Bologna, Italy.

Simona Crea and Nicola Vitiello are with The BioRobotics Institute, Scuola Superiore Sant'Anna, 56025 Pontedera, Italy, also with the Department of Excellence in Robotics and AI, Scuola Superiore Sant'Anna, 56127 Pisa, Italy, and also with IRCCS Fondazione Don Gnocchi, 50143 Florence, Italy.

This article has supplementary downloadable material available at https://doi.org/10.1109/TNSRE.2023.3327751, provided by the authors.

Digital Object Identifier 10.1109/TNSRE.2023.3327751

I. Introduction

LOWER-LIMB prosthetic devices are designed to restore physiological patterns in locomotion activities of daily life by mimicking the torque-angle behaviors of the missing biological joints. As different locomotion activities of daily life require distinct joint patterns, the cognitive human-robot interface (cHRI) of robotic prostheses should be able to decode the users' intent to start, stop, or change locomotion; and select the suitable control strategy, accordingly [1]. The most straightforward approach for cHRIs is requesting manual inputs from the users through physical interfaces such as key fobs [2]. Although this approach is highly reliable, users must stop to give an input command whenever they transition between different locomotion activities. A more intuitive and seamless approach consists of automatically recognizing the users' intent through information provided by the prostheses' sensory systems, in locomotion mode recognition (LMR) algorithms [2].

In the literature, several LMR algorithms were developed and tested with intact [3], [4], [5], [6], [7], [8], [9], [10] and amputee subjects [8], [11], [12], [13], [14], both in offline analyses [5], [7], [12] and real-time applications [3], [4], [6], [11], [14]. The objective of LMR algorithms is to accurately and timely classify the users' activity to avoid mismatches between the action of the device and the users' actual locomotion in terms of modality and temporal onset. The sensory system of LMR algorithms may be composed of: (i) mechanical sensors such as inertial measurement units (IMUs), load cells, goniometers, and encoders [3], [4], [5], [6], [7], [8], [9], [10], [12], [13]; (ii) biosignal sensors, such

as electromyography (EMG) [11]; or (iii) combinations of both [15]. Mechanical sensors, in particular IMUs, have been preferred over EMG sensors to ensure consistent signal quality over time (i.e., reduced need for calibration), as well as less susceptivity to noise, migration of the sensors due to stump-socket interaction forces, and easier donning/doffing of the sensory system [16].

The most frequently used classification algorithms in LMR are Support Vector Machines (SVMs) [3], [6], [7], [15], Hidden Markov Models [4], k-Nearest Neighbors [6], decision trees [8], Linear Discriminant Analysis [12], and Neural Networks [13], [14]. Differently from these algorithms, an alternative approach presented in [5] heuristically classified a step based on its divergence from the templates of the investigated locomotion modes. The templates were constructed as two-dimensional coordinate frames using time-normalized profiles of the thigh angle in the sagittal plane and its mean-subtracted integral. To construct these templates, the profiles must take the form of closed curves with identical initial and end points (as observed in steady-state rhythmic locomotion). This requirement of the closed curves restricts this approach's effectiveness in non-rhythmic movements, such as locomotion mode transitions, and also hinders its ability to detect locomotion modes prior to the completion of a full gait cycle. Another template-based LMR algorithm in [17] used Dynamic Time Warping (DTW) to classify the steps based on their similarity indices with respect to kinematic and inertial signals.

This paper describes an LMR algorithm that uses adaptive Dynamic Movement Primitives (aDMP) as kinematic locomotion templates. aDMP are dynamic systems that can encode the kinematic pattern of a given rhythmic or non-rhythmic movement (namely, within the *movement primitives*) and produce real-time outputs that include estimations of the movement trajectory, target goal (i.e., position at the end of the movement), and continuous movement phase [18]. These variables contain key information about the type of movement that the person is performing; thereby, they can serve as valuable sources to extract features that are useful for locomotion mode recognition without requiring encumbering sensory systems, complex feature engineering, and sophisticated classification algorithms. The proposed algorithm takes accelerometer and gyroscope signals of a thigh-mounted IMU and foot-contact information as inputs to perform discrete classifications during the swing phase, no later than at the end of the current step. In the algorithm framework, predictions are evaluated based on their *confidence* in classification to conclude the algorithm at the earliest moment when an accurate prediction could be made and allocate enough time to a prosthesis to adjust its behavior consecutively. The algorithm was tested on data gathered from ten intact subjects using subject-specific training, as well as on data of a subject with a transtibial amputation during ground-level walking, stair ascending, and stair descending locomotion activities. The steps of these activities were categorized as initiatory, steady-state, and transitory steps.

The main contributions of the proposed algorithm are three folds: (i) aDMP were used for the first time in LMR, (ii) an in-depth consideration of different locomotion modes was investigated, and (iii) to the best of the authors' knowledge, initiatory steps were considered for the first time as a dedicated class.

The rest of the paper is organized as follows: Section II provides a biomechanical analysis of the investigated locomotion modes, elucidating in-between synergies. Section III elaborates on the algorithm architecture's components. Section IV outlines the experimental procedures for intact and transtibial subjects, along with the data processing of the proposed algorithm. Sections V and VI present the acquired results and ensuing discussions, respectively.

II. Biomechanics of the Locomotion Modes

In the categorization of locomotion activities in this work, steady-state and transitory steps are defined as steps in which the locomotion activity is respectively the same and different than that of the previous step. The steady-state steps of stair descending, ground-level walking, and stair ascending, are denoted as SD, GLW, and SA, respectively; whereas, the transitory steps are denoted as SD→GLW, GLW→SD, GLW→SA, and SA→GLW. Finally, initiatory steps refer to the initial steps when transitioning from a standing (ST) position to a locomotion activity. The initiatory steps of the investigated locomotion activities are denoted as ST→SD, ST→GLW, and ST→SA.

Following the definition made in [19], the transitory and initiatory steps were categorized based on whether the transition or initiation was started for the first time by the instrumented or prosthetic leg (called a "leading step") or whether it followed a transition or initiation previously started by the contralateral leg within the same stride (called a "trailing step").

Normative biomechanics data [20], [21], or more explicitly, thigh roll angle during the swing phase of the investigated locomotion modes in this work (Fig. 1) state that GLW, SA, and SD exhibit distinctive kinematic profiles and that the initiatory leading and trailing steps show profiles similar to those of the initiated steady-state locomotion. Similarly, for the trailing transitory steps, the thigh roll angle profiles are similar to those of the upcoming steady-state locomotion whereas, the leading transitory steps show profiles with a more variable behavior, recapped hereafter. In SA→GLW or SD→GLW, the angle profiles resemble those of the previous steady-state locomotion (i.e., SA and SD, respectively) whereas in GLW→SA, the profile resembles that of the upcoming one (i.e., SA). Lastly, in GLW→SD, the profile starts to resemble the upcoming steady-state locomotion (i.e., SD) only after mid-swing.

Based on the similar behavior between leading and trailing initiatory steps, they were considered without this further categorization. Yet, accurate recognition of initiatory steps is critical for the proper actuation of a prosthetic device, without causing users to stop and reinitiate another movement [22]. Thus, initiatory steps were regarded as a separate class and their performance was discussed in the context of adequate and seamless control strategies for robotic prostheses starting from the beginning of a movement. Inversely, steady-state and transitory (both leading and trailing) steps were considered collectively by exploiting their biomechanical relevance, which is hereinafter referred to as *dynamic steps*.

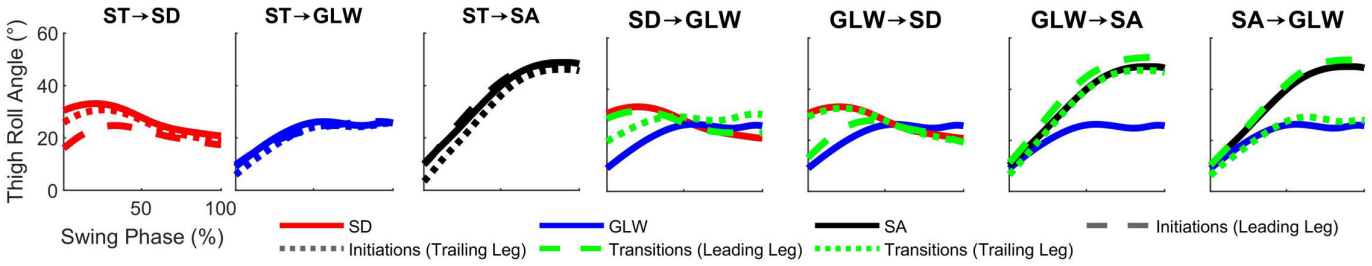

Fig. 1. The thigh roll angles of the initiatory and transitory steps during the swing phase, averaged over the steps of ten intact subjects. For each step, the leading (the dashed lines) and the trailing (the dotted lines) steps are shown separately, along with the related steady-state steps (the solid lines).

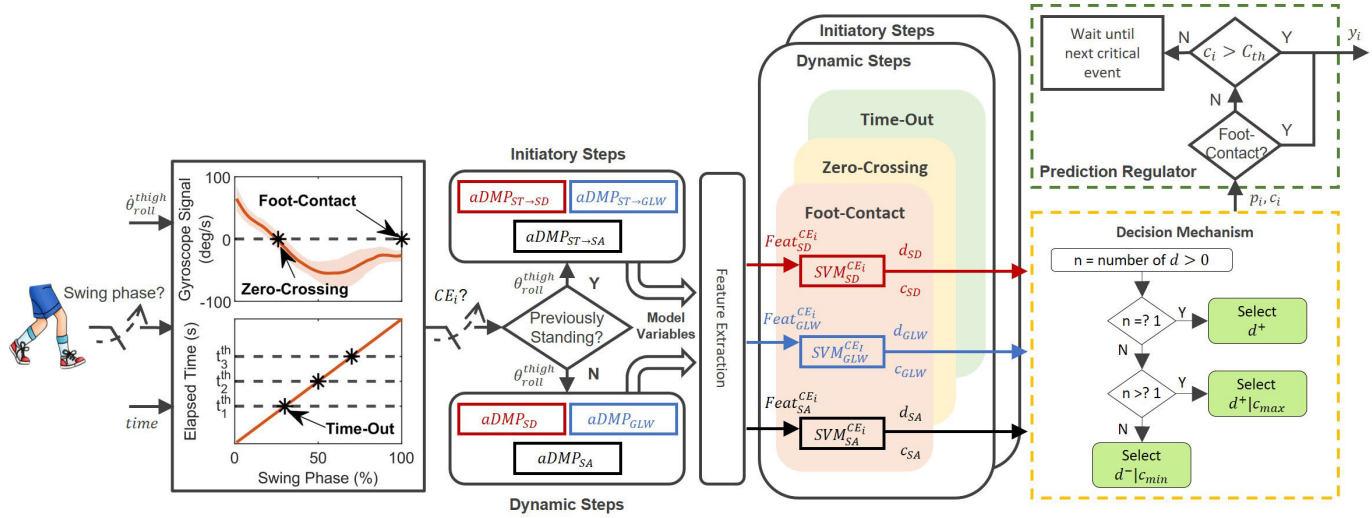

Fig. 2. The general architecture of the proposed algorithm. The users' thigh roll angle, velocity, and the elapsed time are recorded following a foot-off event. Upon detecting a critical event (CE_i), the thigh roll angle is input into a cluster of adaptive Dynamic Movement Primitives (aDMP) models of either initiatory steps (if the user was standing prior to the detected foot-off event) or dynamic steps (if the user was already in motion). As their response to the measured thigh roll angle, these models generate a set of model variables, which are used to extract features for binary Support Vector Machines (SVMs). Three aDMP-SVM pairs run concurrently at a critical event, with SVM outputs (i.e., binary decision *d* and a confidence value *c*) merged in the decision mechanism to produce a prediction *p*. Finally, the predictions at the critical events are combined in the prediction regulator block, allowing the algorithm to terminate as promptly as possible i.e., when the confidence of a prediction satisfies the threshold, before the foot of the sensorized leg touches the ground.

III. Algorithm Architecture

The general architecture of the proposed algorithm is given in Fig. 2. The algorithm is executed at the occurrence of a foot-off event and consists of seven main steps:

Step 1. When the swing phase is detected at the foot off, the algorithm observes the input signals (i.e., the angular velocity of the thigh segment on the sagittal plane $\dot{\theta}\,(i)$, and elapsed time from a foot-off event) to recognize one of the nine critical gait events during the swing phase.

Step 2. When a critical gait event is recognized, the algorithm selects between two paths, the *initiatory* or *dynamic steps* paths, based on whether the user was standing or moving before the foot off.

Step 3. The thigh roll angle is fed to a set of aDMP models, each of which produces a set of model variables.

Step 4. Model variables are used to extract features.

Step 5. The extracted features are input into binary Support Vector Machines (SVMs).

Step 6. The outputs of the SVMs (i.e., binary decision and a confidence value) are combined in a custom decision mechanism.

Step 7. The confidence of the prediction selected by the decision mechanism is used to confirm or deny the prediction at the detected critical event.

The seven steps are described in more detail in the following paragraphs.

A. Critical Events Detection

The classification operations are performed when one of the nine critical gait events is detected during the swing phase. One critical event is detected at foot contact (FC), one at zero crossing (ZC) of the angular thigh velocity in the sagittal plane, and seven are detected at the instances when the time elapsed after foot off exceeds a threshold that ranges from 100ms to 400ms with increments of 50ms (time out, TO).

The FC event acts as a limiting gait event for the prosthesis to execute the classification algorithm and set a proper control strategy at the beginning of the next step, namely at the latest time that allows the prosthesis to have adequate and safe foot-ground interactions. On the other hand, the ZC and TO events are implemented to infer the locomotion mode and adequately control the prosthesis in preparation for the next step before

the next step begins. The TO events are intrinsically affected by the movement speed. To alleviate this speed dependency of the TO events, a wide range of fixed thresholds are included to be evaluated in the prediction regulator.

B. Initiatory/Dynamic Step Detection

The decision node that detects the users' previous status (i.e., whether they are standing or moving) indicates the direction of the aDMP and SVM pairs in the architecture of the algorithm. In the scope of this work (i.e., offline analysis), this decision node was executed by providing information on the step type (i.e., whether a step is dynamic or initiatory) that was pre-defined by the experimenters in the offline segmentation process.

C. Adaptive Dynamic Movement Primitives (aDMP)

This section recaps the main equations of the aDMP model for tracking and prediction of the evolution of discrete monotonic movements, as it was originally formulated [18], and described in the patent application [23]; then presents a generalization of the model to the case of non-monotonic signals, which are present in the investigated locomotion modes of this paper.

The operations of aDMP for monotonic signals can be considered mainly in three folds: (i) offline computation of the movement primitive, (ii) real-time initialization of algorithm variables, and (iii) continuous real-time estimations of trajectory, target goal, and phase.

1) Offline Computation of the Movement Primitive: To compute a movement primitive, first, a single approximated trajectory of the movement, $x(\varphi)$, is defined by approximating a set of its segmented and time-normalized trajectories through N-order Gaussian regression. $x(\varphi)$ is defined as a function of phase, φ, which linearly spans between 0% and 100%. Then, $x(\varphi)$is normalized in amplitude to create a dimensionless trajectory, namely initial movement primitive, denoted as $p_0(\varphi)$:

$$p_0(\varphi) = \begin{cases} \dfrac{x(\varphi) - x_i}{x_f - x_i}, & x_f - x_i > 0 \\ \dfrac{x(\varphi) - x_f}{x_i - x_f}, & x_f - x_i < 0 \end{cases} \tag{1}$$

where x_i and $x_f$correspond to the initial and final values of the created $x(\varphi)$ (i.e., $x_i = x(\varphi = 0\%)$ and $x_f = x(\varphi = 100\%)$), respectively.

Subsequently, a reference target goal θ_{Gref} is defined as:

$$\theta_{Gref} = x_f - x_i \tag{2}$$

2) Real-Time Initialization of Algorithm Variables: At the beginning of a movement in real-time, certain aDMP variables are initialized as described hereinafter.

The target goal estimation, $\hat{\theta}_G$, is initialized as:

$$\hat{\theta}_G(i_0) = \hat{\theta}_{G0} = \theta_0 + \theta_{Gref} \tag{3}$$

where i_0 is the time instance in which the movement begins, and θ_0 is the initial measured trajectory value at i_0.

At the same time, the trajectory estimation, $\hat{\theta}$, is initialized as the initial measured trajectory value:

$$\hat{\theta}(i_0) = \theta_0 \tag{4}$$

Then, the initial forcing term $f_0(\varphi)$ i.e., a function that enforces the progression of the model along the primitive trajectory is calculated as:

$$f_0(\varphi) = \eta^2 \cdot \ddot{y}(\varphi) - \alpha_\omega \cdot \left(\beta_\omega \cdot \left(\hat{\theta}_{G0} - y(\varphi)\right) - \eta \cdot \dot{y}(\varphi)\right) \tag{5}$$

where α_ω, and β_ω are the time constants to imply a monotonic convergence toward the estimated initial target goal, and $y(\varphi)$ is a version of the approximated trajectory that is scaled and offset in amplitude, which is computed as:

$$y(\varphi) = \left|\theta_0 - \hat{\theta}_{G0}\right| \cdot p(\varphi) + \min(\hat{\theta}_{G0}, \theta_0) \tag{6}$$

3) Continuous Real-Time Estimations of Trajectory, Target Goal, and Phase: After initialization, the following operations are performed at each program iteration i, where $i \geq i_0$.

First of all, the normalized trajectory, $\theta_n(i)$, is computed as:

$$\theta_n(i) = \begin{cases} \dfrac{\theta(i) - \theta_0}{\hat{\theta}_G(i) - \theta_0}, & x_f - x_i > 0 \\ \dfrac{\theta(i) - \hat{\theta}_G(i)}{\theta_0 - \hat{\theta}_G(i)}, & x_f - x_i < 0 \end{cases} \tag{7}$$

where $\theta(i)$ and $\hat{\theta}_G(i)$ are the measured trajectory and target goal estimate, respectively.

A continuous real-time phase estimation, $\hat{\varphi}(i)$, is obtained by inverting the movement primitive at iteration i (i.e., $p_i(\varphi)$) with respect to the normalized trajectory, as the phase value that minimizes the difference between $p_i(\varphi)$, and $\theta_n(i)$:

$$\hat{\varphi}(i) = p_i^{-1}(\theta_n(i)) = \text{argmin}_\varphi \left(p_i(\varphi) - \theta_n(i)\right)^2 \tag{8}$$

Secondly, the trajectory value at the next iteration $\hat{\theta}(i+1)$ is estimated using a second-order nonlinear system previously presented in [24]:

$$\hat{\theta}(i+1): \begin{cases} \eta\dot{\hat{\omega}}(i) = \alpha_\omega \left(\beta_\omega \left(\hat{\theta}_G(i) - \hat{\theta}(i)\right) - \hat{\omega}(i)\right) \\ \quad + f_i(\hat{\varphi}(i)) \\ \eta\dot{\hat{\theta}}(i) = \hat{\omega}(i) \end{cases} \tag{9}$$

where $\dot{\hat{\theta}}$ is the time derivative of the estimated trajectory, whereas $\hat{\omega}(i)$ and $\dot{\hat{\omega}}(i)$ are the estimated velocity and its time derivative, respectively.

Finally, a real-time feedback-error term $\epsilon(i)$ is computed as:

$$\epsilon(i) = \theta(i) - \hat{\theta}(i) \tag{10}$$

The feedback error term is used to proportionally update the target goal estimation, movement primitive, and forcing term:

$$\hat{\theta}_G(i+1) = \hat{\theta}_G(i) + K_G \cdot \epsilon(i) \tag{11}$$

$$p_{i+1}(\varphi) = \left(1 + K_p \cdot \epsilon(i)\right) \cdot p_i(\varphi) \tag{12}$$

$$f_{i+1}(\varphi) = \left(1 + K_f \cdot \epsilon(i)\right) \cdot f_i(\varphi) \tag{13}$$

where K_G, K_p, and K_f are gain constants that are tuned to reduce the error term in the next iteration.

4) aDMP Model for Non-Monotonic Signals: The aDMP model is generalized to address non-monotonic inputs by treating them as a series of monotonic regions, each of which is executed in a sequential manner.

Firstly, the approximated trajectory, $x(\varphi)$, is divided into monotonic regions by its extrema during offline computation of the movement primitive. Each monotonic region is identified by a specific initial and final value (i.e., x_i and x_f), and the corresponding phase values (i.e., φ_i and φ_f, respectively). During this stage, a reference target goal and initial movement primitive are also computed for each monotonic region, separately.

In real-time operations, a change in monotonicity is detected if the following condition is met:

$$sign(\theta(i) - \theta(i-1)) \neq sign\left(x_f - x_i\right)$$
$$\left|\varphi_f - \hat{\varphi}(i)\right| \leq \varepsilon_\varphi \hat{\varphi}$$
$$\hat{\varphi}(i) \overset{\wedge}{<} 100\% \tag{14}$$

where ε_φ is the acceptable error bound of the estimated phase to detect a monotonicity change.

Once a change in the monotonicity is detected (if any), the generalized aDMP model proceeds to the next monotonic region, and the operations are repeated from real-time initialization. At this stage, the time instance i_0 is taken as the iteration of the monotonicity change instance.

D. Feature Extraction

A total of 12 features were extracted from aDMP model variables in the temporal window between the foot-off instance and a critical event (TABLE I).

TABLE I
IDENTIFIED SET OF FEATURES

Feature	Description
$RMSE(\hat{\theta}, \theta)$	Position estimation error
$RMSE(\hat{\varphi}, \varphi_{lin})$	Phase estimation error
$RMSE(f_0, f_i)$	Forcing term error
$RMSE(\theta_n, p_i(\hat{\varphi}))$	Normalized position error
$std(\hat{\theta}_G)$	Standard deviation of the estimated target goal
$diff\left(\hat{\theta}_G(i_{ce}), \hat{\theta}_G(i_{fo})\right)$	Difference between the first and the last target goal estimates
$\mu(\hat{\theta})$	Mean of the position estimate
$std(\hat{\theta})$	Standard deviation of the position estimate
$\mu(\hat{\varphi})$	Mean of the phase estimate
$std(\hat{\varphi})$	Standard deviation of the phase estimate
$\mu(f)$	Mean of the forcing term
$std(f)$	Standard deviation of the forcing term

In the table, RMSE stands for root-mean-square error. Moreover, θ and $\hat{\theta}$ represent the measured and estimated positions between foot-off (i.e., i_{fo}) and a critical event (i.e., i_{ce}) instances; $\hat{\varphi}$ and φ_{lin} represent estimated phase and the linear phase; f_0 and f_i represent initial forcing term and forcing term updated in real-time operations; θ_n, p_i, and $\hat{\theta}_G$ represent, normalized position, movement primitive (updated in real-time operations), and estimated target goal, respectively.

E. Support Vector Machines

Features extracted from each aDMP model are fed to a binary SVM with a linear kernel. The choice of the classifiers was motivated by their simple yet performant characteristics [25]. For a given path (i.e., initiatory or dynamic) and a critical event, three SVMs run in parallel to classify the current step following the "one-vs-all" classification approach. In other words, each SVM individually compares the features extracted from one aDMP model (referred to as the positive class) versus the features extracted from the other two models (referred to as the negative class).

The binary decisions, d, of the SVMs are supplemented with a confidence value, c, defined as the perpendicular distance in the z-score-normalized feature space between the trial and the decision boundary that is normalized by the margin of the corresponding classifier.

F. Decision Mechanism

The decision mechanism combines the binary decision of the SVMs and produces a prediction at a critical event. For single-positive decisions (i.e., only one SVM has favored the positive class), the mechanism accepts the decision directly; while for multiple-positive decisions, the prediction is made as the positive decision with the highest confidence. Lastly, in the case of no-positive decisions, the negative decision with the lowest confidence is selected.

G. Prediction Regulator

The role of the prediction regulator is either to accept or reject the output of the decision mechanism based on the associated confidence. Starting from the first detected critical event (i.e., ZC or TO with the lowest threshold) if the confidence of the prediction is higher than the set threshold C_{th}, the prediction is accepted, and the algorithm is concluded for that step. Otherwise, the classification operations are repeated at the following critical event until the confidence of a prediction exceeds the threshold. At the FC event, the prediction is directly accepted.

Three different C_{th} values were investigated in the prediction regulator, which were 0.5, 1, and 2.

IV. MATERIALS AND METHODS

A. Experiments With Human Subjects

Experiments with human subjects are aimed at acquiring a dataset of thigh roll angle profiles in steady-state, transitory, and initiatory steps in all three locomotion activities to validate the LMR algorithm in offline analysis.

Data were acquired from 10 intact participants (9 male, age: 29.7 ± 3.4 years, height: 170.9 ± 3.8 cm, weight: 64.5 ± 5.8 kg) and a subject with transtibial amputation

(male, age: 52, height: 182 cm, weight: 83 kg). All participants provided written informed consent for participating in the study. The experimental protocol on intact participants was approved by the Institutional Review Board of Sant'Anna School of Advanced Studies (approval n. 11/2019) and performed within the premises of Sant'Anna School of Advanced Studies, The BioRobotics Institute (Pontedera, Italy). The study on the transtibial amputee subject was approved by the Area Vasta Toscana Centro Ethics Committee (study number 16678) and conducted at the premises of IRCSS Fondazione Don Carlo Gnocchi (Florence, Italy).

1) Experimental Setups: For intact subjects, the setup consisted of two IMUs, placed frontally on the thighs close to the knee joints by means of elastic bands, and a pair of sensorized shoes. The IMU and sensorized shoe of each leg were processed separately. The IMUs contained a 9-DoF MPU9250 (TDK/InvenSense Inc.) module embedding a three-axis accelerometer, gyroscope, and magnetometer. The accelerometer and gyroscope signals were used to compute the thigh orientation angles, according to Madgwick's algorithm [26]. The sensorized shoes contained 16 pressure-sensitive optoelectronic elements placed on the insoles, and an electronic board for managing data acquisition and wireless communication. The pressure-sensitive elements were used to detect the foot-off and foot-contact events, based on the vertical ground reaction force (vGRF) and center of pressure (CoP) estimates, as presented in [27]. The detected foot-off and foot-contact events enabled and disabled the LMR algorithm. The signals were wirelessly acquired by a National Instruments sbRIO-9651, in real-time with a sampling frequency of 100 Hz.

The transtibial amputee subject was requested to wear the Wearable Robotics Laboratory TransTibial Prosthesis (WRL TTP), a semi-active ankle-foot prosthesis designed to enhance the push-off during walking [28]. During experimentations, the WRL TTP did not provide additional power to the user and acted as a passive energy-storage-and-return foot. The sensory system of the prosthesis included an on-board IMU located at the shank (iNemo, LSM9DS1, STMicroelectronics), and two wired IMUs (MPU9250, TDK/InvenSense Inc.) placed on the back of the prosthetic foot and frontally on the thigh of the residual limb close to the knee joint, a sensorized prosthetic foot equipped with 16 pressure-sensitive elements attached under the sole. The thigh IMU was used for offline analysis of the LMR algorithm, whereas the foot IMU or the sensorized foot was used for detecting the foot-off and foot-contact events through measured acceleration and angular velocity or estimated vGRF values, as described in [29]. The signals were acquired via an embedded National Instruments sbRIO-9651 module at 100 Hz.

2) Experimental Protocols: The subjects were helped in placing and fastening the sensory systems. In the case of the amputee subject, a professional prosthetist fitted the prosthesis to ensure its correct alignment. Before the experimental sessions, subjects underwent a calibration process to offset the signal readings of the sensors.

The intact subjects were requested to perform the following movement sequence with their natural gait pattern: walk 6 meters from a standing-still initial position, climb a staircase of 11 steps, walk a short landing (1 meter), climb another staircase of 11 steps, walk over ground level for another 6 meters, stop, turn around, and repeat the sequence in the reverse order. During staircase ascending and descending, subjects were asked to stop and transition to standing condition for approximately 2 seconds in the middle of each set of stairs. The experimental circuit was repeated three times with different self-selected cadences (i.e., normal, low, and very low). All three cadences were included in the dataset to study the robustness of the algorithm to temporal variances.

The subject with transtibial amputation performed the following movement sequence at his self-selected comfortable speed: walk approximately 3 meters starting from a standing position, climb up a two-sided 3-step staircase, stop at the top for approximately 2 seconds, climb down the stairs on the other side, walk again approximately 3 meters before stopping, turning around, and repeating the movements in the reverse direction. The described sequence was repeated a total of 32 times. In 16 of these repetitions, the subject was asked to stop and stand for approximately 2 seconds before transitioning to another locomotion activity for the collection of the initiatory steps, while in the other 16 repetitions, the transitions between locomotion modes were continuous for the collection of transitory steps.

In experiments with the intact subjects or the transtibial amputee, the data were labeled in real-time by the experimenters and corrected manually in postprocessing. Subjects performed the initiatory and transitory movements with their preferred leg. Due to the limitations of the experimental setup, particularly the staircase structure, the transtibial amputee data contain only SD→GLW and GLW→SA transitory steps.

B. Dataset Generation

The acquired data were segmented in postprocessing according to the foot-off and foot-contact information obtained in real time. The dataset contained an abundant amount of GLW, compared to SA and SD. To balance the dataset, we reduced the number of GLW steps by random selection. The size of the dataset is available in Supplementary Materials.

C. Algorithm Training and Testing

The dataset of each subject was split into training and test sets following a 5-fold cross-validation. At each fold, 5 thigh roll angle trajectories were randomly selected from the training sets to compute the movement primitives for the aDMP models. The remaining samples were used to compute features, which were z-score normalized before training the SVM classifiers. Trials that contained at least one feature beyond $\pm$ 5 standard deviations were treated as outliers and excluded during training.

For the *dynamic steps* pathway, the computation of the movement primitives and the training of the SVMs were performed using only steady-state steps, and the transitory steps were used solely as test samples. For the classification, the transitory steps were relabeled with pseudo-steady-state labels, as reported in TABLE II, based on the biomechanical analysis presented in Section II.

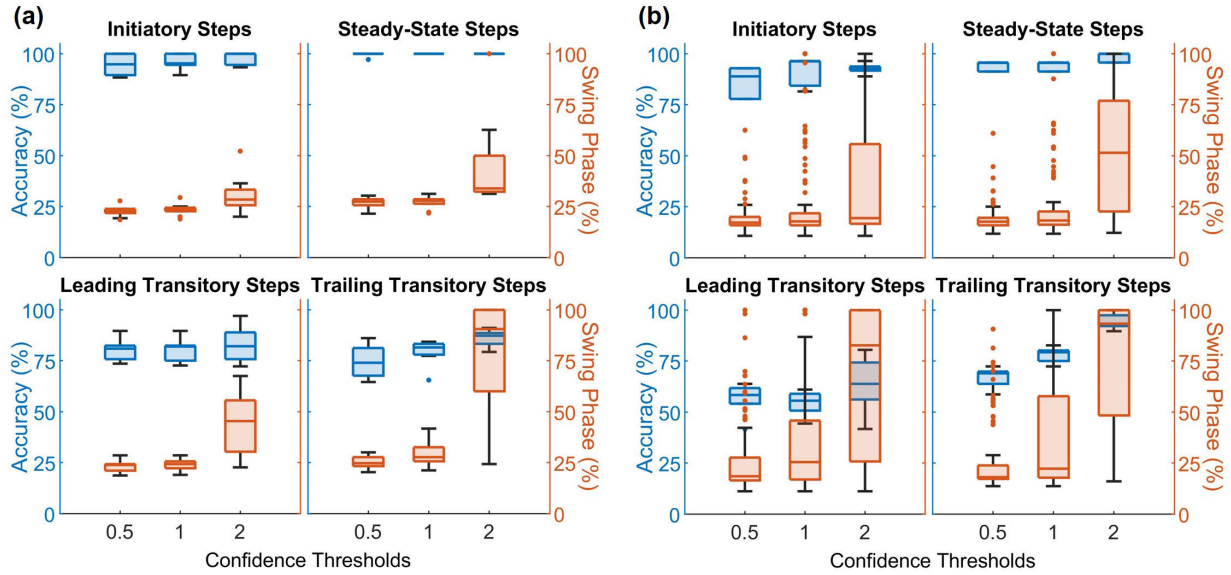

Fig. 3. The classification accuracies (in blue) and classification onsets (in red) of the (a) ten intact participants and (b) subject with transtibial amputation, given for different confidence thresholds of the prediction regulator. The classification onsets signify the instances in which the classification operations commence and are reported as percentage of the swing phase. In (a), the results present the spread across intact participants, whose individual performance were assessed across cross validation folds. In (b), the results present the spread across cross validation folds of the subject with transtibial amputation.

TABLE II
PSEUDO-STEADY-STATE LABELS OF THE TRANSITORY STEPS

Transitory Modes	Leading Steps	Trailing Steps
SD→GLW	SD	GLW
GLW→SD	SD	SD
GLW→SA	SA	SA
SA→GLW	SA	GLW

The abbreviated locomotion activities correspond to stair descending (SD), ground-level walking (GLW), and stair ascending (SA).

D. Performance Evaluation

The proposed algorithm was developed and tested using MATLAB R2020a (MathWorks, Inc., Natick, MA, USA). The algorithm was evaluated in terms of accuracy and time of the classification onset (i.e., the time instant in which feature computation and subsequent classification operations commence). The classification onset is expressed as the percentage of the duration of the swing phase.

The performance of the algorithm was assessed in terms of median values since the distributions of the performance indices failed the Anderson-Darling normality test at the significance level of 5%.

V. RESULTS

A. Intact Participants

The performance of the LMR algorithm with data from intact participants are presented in Fig. 3a. Overall, initiatory steps were classified with 94.74%, 95.23%, and 100% median accuracies at medially 22.73%, 23.39%, and 28.45% of the swing phase for the confidence thresholds of 0.5, 1, and 2- respectively.

Steady-state steps were correctly classified (i.e., 100% median accuracies) for all the confidence thresholds. The median classification onsets of steady-state steps were obtained as 27.40% of the swing phase for $C_{th} = 0.5$, 27.78% for $C_{th} = 1$, and 33.87% for $C_{th} = 2$.

The median accuracies for the leading transitory steps were 80.91%, 81,98%, 82.16%, which were obtained at medially 23.81%, 24.39%, and 45.34% of the swing phase for the thresholds of 0.5,1, and 2- respectively. Lastly, the trailing transitory steps resulted in the median accuracies of 74.08%, 81.50%, and 87.30% at medially 24.7%, 27.66%, and 90.54% of the swing phase.

The confusion matrices of initiatory, steady-state, and transitory (leading and trailing) steps of the intact subjects are shown in Fig. 4a for the confidence threshold of 2. The leading GLW→SD, trailing SD→GLW, and SA→GLW steps were noted to be the most confused locomotion modes.

Additional results on the intact subjects, such as the individual performances of the critical events without the prediction regulator, and selected critical events in the prediction regulator are available in Supplementary Materials.

B. Amputee Participant

The accuracies and classification for the transtibial amputee patient are presented in Fig. 3b. Initiatory steps were classified with 88.89%, 96.30%, and 92.59%% median accuracies medially at 17.24%, 17.86%, and 19.48% of the swing phase for the confidence thresholds of 0.5, 1, and 2- respectively.

The stead-state steps were classified with a median accuracy of 95.45% for the certainty thresholds of 0.5 and 1 medially at 17.70% and 18.18% of the swing phase, and with 100.0% median accuracy for the confidence threshold of 2, medially at 51.47% of the swing phase.

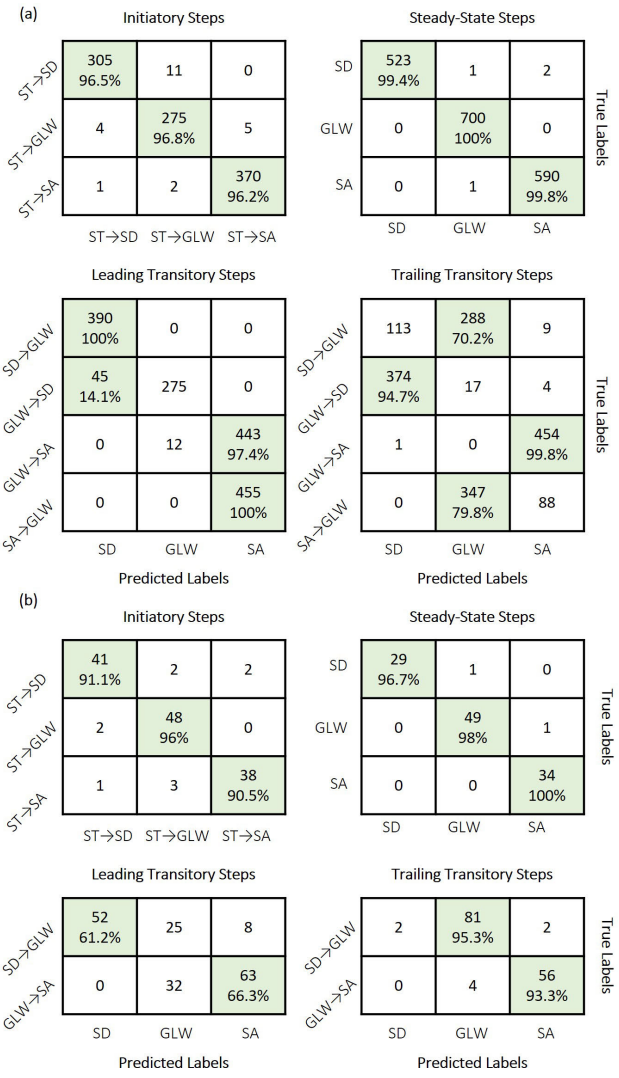

Fig. 4. The confusion matrices for different step types of the (a) intact subjects, and (b) subject with transtibial amputation, given for the confidence threshold of 2. The matrices show the accumulated test trials across subjects and validation folds in (a), and across validation folds in (b). The true positives are highlighted in green and provided with the true positive rates. The true positives for transitory steps (leading and trailing) are assigned according to pseudo-labelling presented in TABLE II. The transitory steps of the subject with transtibial amputation contain only SD→GLW and GLW→SA modes due to limitations of the experimental setup.

Lastly, the leading transitory steps were classified with the median accuracies of 58.33%, 55.56%, and 63.89% medially at 18.52%, 25.43%, and 82.68% of the swing phase for the confidence thresholds of 0.5, 1, and 2- respectively. The trailing transitory steps were classified with the median accuracies of 68.97%, 79.31%, and 93.10%; and the classification onsets were obtained as 18.18%, 22.22%, and 93.33% of the swing phase for the confidence thresholds of 0.5, 1, and 2 respectively.

The confusion matrices of initiatory, steady-state, and transitory (leading and trailing) steps of the subject with a transtibial amputation are shown in Fig. 4b for the confidence threshold of 2. Leading transitory steps were the most confused locomotion modes. Additional results on the amputee subject are available in Supplementary Materials.

VI. Discussion

A. Intact Participants

In all the locomotion except steady-state, increasing confidence thresholds resulted in improved classification accuracies at the cost of delayed classification onset, since the algorithm is designed to wait until a critical event that shows high confidence, which often happens at later stages of the swing phase.

The individual performance of the TO and ZC critical events showed similar accuracies compared to the FC event for the initiatory, steady-state, and leading transitory steps, while for the trailing transitory steps, the TO events with low thresholds were less performant (see Supplementary Materials Section B). Furthermore, the TO event with the 100ms threshold (TO100) was the earliest-occurring critical event for most cases, which also was the most selected critical event by the prediction regulator, particularly for the confidence thresholds of 0.5 and 1 (see Supplementary Materials Section C). As a result, five-fold cross-validated initiatory, steady-state, and leading trailing steps were classified with high accuracies at the early stages of the swing phase. On the contrary, the trailing transitory steps were best classified in later instances.

Overall, the initiatory and steady-state steps were classified with higher accuracies compared to the transitory steps. This could be explained by the absence of the transitory steps in the training sets. Hence, the accuracies of the transitory steps might be increased if their trials are included in the computation of the movement primitives of the aDMP models and the training of the SVMs for the *dynamic steps* pathway. Alternatively, the low accuracies of the transitory steps might indicate the need for a dedicated classification. However, this would require an additional module to distinguish between the transitory and steady-state steps, which might accumulate errors and delay the classification in real-time operations.

In this work, the classification of the locomotion mode of transitory and steady-state steps leveraged the inherent biomechanical similarities between these two step types, without the need for prior differentiation. This approach has demonstrated its effectiveness in handling transitions between SA and GLW by accurately inferring the correct operation mode for a prosthetic device. However, classification based on biomechanical relevance may not be as straightforward when dealing with transitions between SD and GLW. In the case of leading SD→GLW steps, the pseudo-label was assigned as SD from the biomechanical analysis. Considering the SD pseudo-label, the algorithm classified these transitory steps with high accuracy (e.g., 100% for the confidence threshold of 2), which supports the validity of biomechanical relevance in LMR applications. In the step succeeding the leading SD→GLW transitions, the joint kinetic and kinematic profiles closely resemble SD during the stance phase of the ankle and the early-stance phase of the knee [19]. Hence, this classification would enable the implementation of appropriate control strategies for an active ankle prosthesis in the subsequent step by mimicking the torque-angle profile of the biological ankle joint. It would further ensure safe weight acceptance for an active knee prosthesis. A different situation occurs for leading

TABLE III
SUMMARY OF RELEVANT WORKS IN THE LITERATURE

Paper	Subject Number (Type)	Sensor Type (Position)	Locomotion Activities	Method	Accuracy(Prediction Moment)	
					Steady-State	Transitions
This Work	10 (I)	1 IMU (thigh) and Pressure-Sensitive Insoles	GLW, SA, SD	aDMP-based SVM	100% (27.40% of swing)	82.16% (Leading) (45.34% of swing) 87.30% (Trailing) (90.54% of swing)
	1 (TT)				100% (51.47% of swing)	63.89% (Leading) (82.68% of swing) 93.10% (Trailing) (93.33% of swing)
[4]	10 (I)	1 IMU (shoe)	GLW, SA, SD, R	TMC-HIST	99.20% (Not Available)	Not Available
[5]	7 (I)	1 IMU (thigh)	GLW, SA, SD	Phase-variable-based Templates	99.4% (FC)	~99% (≥1 step delay)
[6]	6 (I)	1 IMU (thigh)	GLW, SA, SD, J	k-Nearest Neighbors	92.3% (around mid-swing)	100% (1 step delay)
				SVM	93% (around mid-swing)	100% (1 step delay)
[7]	10 (I)	1 IMU (thigh) and Pressure-Sensitive Insoles	GLW, SA, SD	DAG-based SVM	98.7% (75% of stride)	95.6% (85% of stride)
[8]	3 (I)	1 IMU (foot)	GLW, SA, SD, RA, RD	Decision Tree	98.6% (< 90±56ms)	Not Available
	3 (TT)				98.4% (<105 ± 66ms)	Not Available
[9]	8 (I)	3 IMUs (thigh, shank, foot)	GLW, RA, RD	Bayesian Classifier	99.87% (Not Available)	Not Available
[10]	6 (I)	2 Encoders (hip) and 2 Pressure-Sensitive Insoles	GLW, SA, SD, ST, Sit,	Rule Based + Fuzzy Logic Classifier	99.4% (Not Available)	Reported together with steady-state
[12]	6 (TT)	1 IMU (shank)	GLW, SA, SD, RA, RD	Linear Discriminant Analysis	up to ~98% (no later than FC)	up to ~95% (no later than FC)
[13]	3 (TT)	1 Strain Gauge (prosthetic foot)	GLW, SA, SD, RA, RD	Convolutional Neural Networks	89.11% (FC)	Not Available
			GLW, A (SA and RA), D (SD and RD)		92.53% (FC)	Not Available
[14]	3 (TT)	2 IMUs (shank and foot)	GLW, SA, SD, RA, RD	Neural Network	96.72% (Not Available)	Not Available
[17]	6 (TT)	2 IMUs (shank and foot) and 1 Pressure Sensor (insole)	GLW, SA, SD, RA, RD	Dynamic Time Warping	96.2% (Not Available)	Not Available

I = Intact Subject, TT = Transtibial Amputee Subject, IMU = Inertial Measurement Unit, GLW = Ground-Level Walking, SA = Stair Ascend, SD = Stair Descend, R = Running, J = Jogging, RA = Ramp Ascend, RD = Ramp Descend, ST = Standing, Sit = Sitting, aDMP = adaptive Dynamic Primitives, TMC-HIST = Triplet Markov Chain Model with Histograms, SVM = Support Vector Machine, DAG = Directed Acyclic Graphs, GMM = Gaussian Mixture Model, FC = Foot Contact

GLW→SD steps. In this case, the knee and ankle profiles in the next step are similar to SD [19], leading to the assignment of the SD pseudo-label. Nevertheless, the algorithm misclassified these transitory steps as GLW, mainly due to the resemblance of the thigh roll angle to GLW in the early swing phase. Although this misclassification would not be ideal for prosthesis control, it should be noted that the higher quasi-stiffness of the knee and ankle joints in GLW would still ensure good support during the critical weight-acceptance phase following transitory GLW→SD steps [19].

The previous works on LMR algorithms tested with intact subjects are presented in TABLE III. Only studies that achieved accuracies above 99% in steady-state locomotion have been included. To the best of the authors' knowledge, the recognition of initiatory steps was not explicitly included in the current LMR algorithms, instead, specific initiatory steps were considered as a part of transitory steps. For instance, ST→SA and ST→GLW steps were classified with the overall accuracies of 91.7%, and 96.4%, using two IMUs (located at the shank and foot segments) and a pressure-sensitive insole in [30]. And, in [31], ST→SA and ST→SD steps were classified with accuracies up to 99.97% and 99.08%, respectively, using a total of 18 mechanical sensors embedded in the prosthesis.

In this work, steady-state locomotion modes were recognized with comparably high accuracies and early classification onsets with respect to other works in the literature. On the other hand, comparing the outcomes of the proposed algorithm with those of other studies for the transitory steps is intricate, primarily due to the lack of detailed distinction between leading and trailing steps. Motivated by the fact that the biomechanical profiles and subsequent control requirements differ for leading and trailing transitory steps as demonstrated in this work, such detailed consideration of transitory steps could offer a guiding framework to fellow researchers in future studies. Nevertheless, the proposed

algorithm resulted in accuracies that were closely aligned with prior research findings for five out of eight transitions (e.g., leading SD→GLW, SA→GLW, and GLW→SA; or trailing GLW→SD and GLW→SA steps). It is also worth noting that several studies either did not specify the classification timings or experienced considerable delays (i.e., a step or more), potentially posing safety concerns in real-world applications. Lastly, comparable performance was achieved with the current state-of-the-art for the initiatory steps by using a smaller number of sensors, despite the similar lack of differentiation between leading and trailing steps in the existing literature.

B. Amputee Participant

The individual performance of the critical events was similar for the initiatory and steady-state steps (see Supplementary Materials Section B). The TO100 event also resulted as the earliest-occurring critical event, whereas the ZC event for the amputee participant occurred considerably later compared to the intact group. The predictions made at 100ms were effective in concluding the algorithm, particularly for the confidence threshold of 0.5 and 1. On the other hand, the transitory steps were classified with better accuracies at later stages of the swing phase, however, the prediction regulator still chose the TO100 event to conclude the algorithm for the confidence thresholds of 0.5 and 1 (see Supplementary Materials Section C), resulting in lower accuracies compared to the threshold of 2.

The initiatory and steady-state steps of the amputee subject showed minor misclassifications, which were in line with the results of the intact subjects. On the other hand, its leading transitory steps showed an increased number of misclassifications while its trailing transitory steps performance was improved compared to the intact participants. Again, the accuracy of the transitions (particularly the leading steps) could be improved if they are included in the computation of the movement primitives in aDMP models and training of the SVMs.

The previous works on LMR algorithms involving transtibial subjects are reported in TABLE III. The proposed algorithm obtained results comparable to the current literature for steady-state steps. Only one study reported performance on transitory steps [12], whose performance were also comparable with this paper. Lastly, initiatory steps were not previously considered for participants with transtibial amputation. The limited literature on the systematic evaluation of transitory and initiatory steps highlights the need for further investigation in this area.

The proposed algorithm was originally designed with an exclusive consideration of intact subjects. Then, it was applied to the transtibial amputee data as a preliminary investigation towards the end-users of LMR architectures. Therefore, the performance obtained here for the single amputee subject could be improved if certain aspects of the algorithm (e.g., the identified features, and the definition of the critical events) are revised accordingly to the amputee-specific locomotion characteristics.

C. Limitations and Future Works

The main limitation of this work is the lack of a real-time evaluation. Particularly, the user perception of the misclassified leading transitory steps between GLW and SD, as well as their impact on overall prosthetic control require further human-in-the-loop assessments by integrating this algorithm with adequate controllers. In such a setting, countermeasure loops could be implemented in the software to allow the subjects to override the algorithm's decision, for instance by relieving the weight on the prosthetic side to drive the prosthesis to a safety mode (e.g., locking the joints). Moreover, human-in-the-loop studies are paramount to evaluate whether the classification onsets shown in this work are sufficient to control a prosthesis in real time, considering controller latencies. This is more crucial for certain initiatory and transitory steps (e.g., ST→SA or GLW→SA), in which it is desirable to change the device behavior at earlier instances of the gait (e.g., before encountering the step rise) to avoid safety risks. Lastly, the scalability of this algorithm will be investigated using generalized movement primitives and classifiers, involving more intact and amputee subjects.

Acknowledgment

The authors would like to thank Tommaso Ciapetti, Alessandro Maselli, Erika Guolo, and Prof. Raffaele Molino Lova from IRCSS Fondazione Don Carlo Gnocchi (Florence, Italy) for their contribution during the experimental sessions. The authors also declare that Simona Crea and Nicola Vitiello have commercial interests in IUVO S.r.l., a spinoff company of Scuola Superiore Sant'Anna. Currently, the IP protecting the adaptive Dynamic Movement Primitives algorithm has been licensed to IUVO S.r.l.

References

[1] M. R. Tucker et al., "Control strategies for active lower extremity prosthetics and orthotics: A review," *J. NeuroEngineering Rehabil.*, vol. 12, no. 1, p. 1, 2015, doi: 10.1186/1743-0003-12-1.

[2] T. Lenzi and L. Hargrove, "User-adaptive control of robotic lower limb prostheses," in *Proc. Encyclopedia Med. Robot.*, Nov. 2018, pp. 89–110, doi: 10.1142/9789813232327_0004.

[3] Z. Zhou, X. Liu, Y. Jiang, J. Mai, and Q. Wang, "Real-time onboard SVM-based human locomotion recognition for a bionic knee exoskeleton on different terrains," in *Proc. Wearable Robot. Assoc. Conf. (WearRAcon)*. Piscataway, NJ, USA: Institute of Electrical and Electronics Engineers, Nov. 2019, pp. 34–39, doi: 10.1109/WEARRACON.2019.8719399.

[4] H. Li, S. Derrode, and W. Pieczynski, "An adaptive and on-line IMU-based locomotion activity classification method using a triplet Markov model," *Neurocomputing*, vol. 362, pp. 94–105, Oct. 2019, doi: 10.1016/j.neucom.2019.06.081.

[5] H. L. Bartlett and M. Goldfarb, "A phase variable approach for IMU-based locomotion activity recognition," *IEEE Trans. Biomed. Eng.*, vol. 65, no. 6, pp. 1330–1338, Jun. 2018, doi: 10.1109/TBME.2017.2750139.

[6] P. T. Chinimilli, S. Redkar, and T. Sugar, "A two-dimensional feature space-based approach for human locomotion recognition," *IEEE Sensors J.*, vol. 19, no. 11, pp. 4271–4282, Jun. 2019, doi: 10.1109/JSEN.2019.2895289.

[7] V. Papapicco et al., "A classification approach based on directed acyclic graph to predict locomotion activities with one inertial sensor on the thigh," *IEEE Trans. Medical Robot. Bionics*, vol. 3, no. 2, pp. 436–445, May 2021, doi: 10.1109/TMRB.2021.3075096.

[8] F. Gao, G. Liu, F. Liang, and W.-H. Liao, "IMU-based locomotion mode identification for transtibial prostheses, orthoses, and exoskeletons," *IEEE Trans. Neural Syst. Rehabil. Eng.*, vol. 28, no. 6, pp. 1334–1343, Jun. 2020, doi: 10.1109/TNSRE.2020.2987155.

[9] U. Martinez-Hernandez, I. Mahmood, and A. A. Dehghani-Sanij, "Simultaneous Bayesian recognition of locomotion and gait phases with wearable sensors," *IEEE Sensors J.*, vol. 18, no. 3, pp. 1282–1290, Feb. 2018, doi: 10.1109/JSEN.2017.2782181.

[10] A. Parri et al., "Real-time hybrid locomotion mode recognition for lower limb wearable robots," *IEEE/ASME Trans. Mechatronics*, vol. 22, no. 6, pp. 2480–2491, Dec. 2017, doi: 10.1109/TMECH.2017.2755048.

[11] M. Liu, F. Zhang, and H. Huang, "An adaptive classification strategy for reliable locomotion mode recognition," *Sensors*, vol. 17, no. 9, p. 2020, Sep. 2017, doi: 10.3390/s17092020.

[12] R. Stolyarov, G. Burnett, and H. Herr, "Translational motion tracking of leg joints for enhanced prediction of walking tasks," *IEEE Trans. Biomed. Eng.*, vol. 65, no. 4, pp. 763–769, Apr. 2018, doi: 10.1109/TBME.2017.2718528.

[13] Y. Feng, W. Chen, and Q. Wang, "A strain gauge based locomotion mode recognition method using convolutional neural network," *Adv. Robot.*, vol. 33, no. 5, pp. 254–263, Mar. 2019, doi: 10.1080/01691864.2018.1563500.

[14] D. Xu and Q. Wang, "BP neural network based on-board training for real-time locomotion mode recognition in robotic transtibial prostheses," in *Proc. IEEE Int. Conf. Intell. Robots Syst.*, Nov. 2019, pp. 8158–8163, doi: 10.1109/IROS40897.2019.8968298.

[15] F. Barberi et al., "Early decoding of walking tasks with minimal set of EMG channels," *J. Neural Eng.*, vol. 20, no. 2, Apr. 2023, Art. no. 026038, doi: 10.1088/1741-2552/ACC901.

[16] F. Labarrière et al., "Machine learning approaches for activity recognition and/or activity prediction in locomotion assistive devices—A systematic review," *Sensors*, vol. 20, no. 21, p. 6345, Nov. 2020, doi: 10.3390/S20216345.

[17] E. Zheng, Q. Wang, and H. Qiao, "An automatic labeling strategy for locomotion mode recognition with robotic transtibial prosthesis," in *Proc. IEEE 9th Annu. Int. Conf. CYBER Technol. Autom., Control, Intell. Syst. (CYBER)*, Jul. 2019, pp. 1010–1013, doi: 10.1109/CYBER46603.2019.9066503.

[18] F. Lanotte, Z. McKinney, L. Grazi, B. Chen, S. Crea, and N. Vitiello, "Adaptive control method for dynamic synchronization of wearable robotic assistance to discrete movements: Validation for use case of lifting tasks," *IEEE Trans. Robot.*, vol. 37, no. 6, pp. 2193–2209, Dec. 2021, doi: 10.1109/tro.2021.3073836.

[19] M. Grimmer et al., "Lower limb joint biomechanics-based identification of gait transitions in between level walking and stair ambulation," *PLoS ONE*, vol. 15, no. 9, Sep. 2020, Art. no. e0239148, doi: 10.1371/journal.pone.0239148.

[20] G. Bovi, M. Rabuffetti, P. Mazzoleni, and M. Ferrarin, "A multiple-task gait analysis approach: Kinematic, kinetic and EMG reference data for healthy young and adult subjects," *Gait Posture*, vol. 33, no. 1, pp. 6–13, Jan. 2011, doi: 10.1016/j.gaitpost.2010.08.009.

[21] D. A. Winter, "Energy generation and absorption at the ankle and knee during fast, natural, and slow cadences," *Clin. Orthopaedics Rel. Res.*, vol. 175, pp. 147–154, Nov. 1983, doi: 10.1097/00003086-198305000-00021.

[22] D. Novak et al., "Automated detection of gait initiation and termination using wearable sensors," *Med. Eng. Phys.*, vol. 35, no. 12, pp. 1713–1720, Dec. 2013, doi: 10.1016/j.medengphy.2013.07.003.

[23] N. Vitiello, F. Lanotte, and S. Crea, "A method for the adaptive control of a wearable robot, such as an orthesis or a prosthesis, and wearable robot operating according such method," WO 2 019 073 407, Oct. 12, 2017.

[24] A. J. Ijspeert, J. Nakanishi, H. Hoffmann, P. Pastor, and S. Schaal, "Dynamical movement primitives: Learning attractor models for motor behaviors," *Neural Comput.*, vol. 25, no. 2, pp. 328–373, Feb. 2013, doi: 10.1162/NECO_a_00393.

[25] D. A. Pisner and D. M. Schnyer, "Support vector machine," in *Machine Learning: Methods and Applications to Brain Disorders*. New York, NY, USA: Academic Press, Nov. 2019, pp. 101–121, doi: 10.1016/B978-0-12-815739-8.00006-7.

[26] S. O. H. Madgwick. (2010). *An Efficient Orientation Filter for Inertial and Inertial/Magnetic Sensor Arrays*. Report X-IO and University. [Online]. Available: http://sharenet-wii-motion-trac.googlecode.com/files/An_efficient_orientation_filter_for_inertial_and_inertialmagnetic_sensor_arrays.pdf

[27] E. Martini et al., "Pressure-sensitive insoles for real-time gait-related applications," *Sensors*, vol. 20, no. 5, p. 1448, Mar. 2020, doi: 10.3390/s20051448.

[28] A. Mazzarini et al., "A low-power ankle-foot prosthesis for push-off enhancement," *Wearable Technol.*, vol. 4, Jun. 2023, doi: 10.1017/WTC.2023.13.

[29] T. Fiumalbi et al., "A multimodal sensory apparatus for robotic prosthetic feet combining optoelectronic pressure transducers and IMU," *Sensors*, vol. 22, no. 5, p. 1731, Feb. 2022, doi: 10.3390/S22051731.

[30] A. Parri et al., "Whole body awareness for controlling a robotic transfemoral prosthesis," *Frontiers Neurorobotics*, vol. 11, p. 25, May 2017, doi: 10.3389/fnbot.2017.00025.

[31] A. M. Simon et al., "Delaying ambulation mode transition decisions improves accuracy of a flexible control system for powered knee-ankle prosthesis," *IEEE Trans. Neural Syst. Rehabil. Eng.*, vol. 25, no. 8, pp. 1164–1171, Aug. 2017, doi: 10.1109/TNSRE.2016.2613020.

Open Access funding provided by 'Scuola Superiore "S.Anna" di Studi Universitari e di Perfezionamento' within the CRUI CARE Agreement